Received April 27, 2020, accepted May 11, 2020, date of publication May 18, 2020, date of current version June 1, 2020.

Digital Object Identifier 10.1109/ACCESS.2020.2995170

Distributed Error Correction of EKF Algorithm in Multi-Sensor Fusion Localization Model

FENGJUN HU[1] AND GANG WU[2]

[1]Institute of Information Technology, Zhejiang Shuren University, Hangzhou 310015, China

[2]Department of Oral Implantology and Prosthetic Dentistry, Academic Centre for Dentistry Amsterdam (ACTA), University of Amsterdam (UvA) and Vrije Universiteit Amsterdam (VU), 1081LA Amsterdam, The Netherlands

Corresponding author: Fengjun Hu (hufengjun@zjsru.edu.cn)

This work was supported in part by the National Natural Science Foundation of China under Grant 51675490 and Grant 81911530751, in part by the Natural Science Foundation of Zhejiang Province under Grant LGG20F020015, and in part by the Young Academic Team Project of Zhejiang Shuren University.

ABSTRACT In order to solve the problem that the standard extended Kalman filter (EKF) algorithm has large errors in Unmanned Aerial Vehicle (UAV) multi-sensor fusion localization, this paper proposes a multi-sensor fusion localization method based on adaptive error correction EKF algorithm. Firstly, a multi-sensor navigation localization system is constructed by using gyroscopes, acceleration sensors, magnetic sensors and mileage sensors. Then the information detected by the sensor is compared and adjusted, to reduce the influence of error on the estimated value. The nonlinear observation equation is linearized by Taylor, and the normal distribution hypothesis is carried out in two steps of prediction and correction respectively. Finally, the parameters of system noise and measurement noise covariance in EKF are optimized by using the evolutionary iteration mechanism of genetic algorithm. The adaptive degree is obtained according to the absolute value of the difference between the estimated value and the real value of EKF. The individual evaluation results of EKF algorithm parameters are used as the measurement standard for iteration to obtain the optimal value of EKF algorithm parameters. Experimental simulation results show that the improved algorithm proposed has higher real-time localization accuracy and higher robustness than those of the standard EKF algorithm.

INDEX TERMS EKF algorithm, smart sensing, distributed error correction, parameter optimization, multi-sensor fusion, Internet of Things.

I. INTRODUCTION

Location Based Services (LBS) is a basic service that obtains the current location and provides information resources through various mobile location technologies [1]–[3]. At present, the most basic localization technology generally uses GPS sensors for real-time localization, but GPS signals are easily blocked, or interfered, thus high-precision localization cannot be realized [4]–[6]. Therefore, based on a single data source, many research institutions, universities, etc. use multi-source sensor data fusion to complement each other's advantages and realize accurate localization [7]–[9].

The common multi-sensor fusion localization method is to collect real-time data of gyroscopes, acceleration sensors, magnetic sensors, mileage sensors, inertial measurement units, vision sensors and other sensors, and to use data fusion for high-precision localization. Ghosh *et al.* [10] used wheel tester, inertial measurement unit and rotating 2D laser scanner to locate and correct the mobile robot in real time. Nada *et al.* [11] took odometer, magnetic compass and acceleration sensor data as inputs of Unscented Kalman Filter (UKF) to realize data fusion and real-time localization. Belmonte-Hernández *et al.* [12] proposed a multi-sensor fusion adaptive fingerprint (MUFAF) algorithm, which uses interpolation to improve the responsiveness of the algorithm to the environment. Shivanand *et al.* [13] proposed an asynchronous multi-rate multi-sensor state vector fusion algorithm, which optimizes the localization accuracy by eliminating the coupling between covariance terms. Muniandi and Deenadayalan [14] used wheeled sensors, radar and GNSS as data acquisition sensors, and constructed a

The associate editor coordinating the review of this manuscript and approving it for publication was Rongbo Zhu.

nonlinear real-time localization model by probability weighting method. Al-Sharman *et al.* [15] used Kalman innovation sequence and covariance matching technology to continuously adjust through fuzzy inference system, and proposed real-time localization based on adaptive fuzzy Kalman fusion algorithm (AFKF). Plangi *et al.* [16] proposed a real-time localization algorithm based on Kalman filter algorithm to solve the routing problem in real-time localization. Kumar and Hegde [17] established a multi-sensor combined attenuation model and adopted joint error optimization for multi-sensor data to reduce localization error. Gabela *et al.* [18] used GNSS and LPS as data sources and improved the localization accuracy by combining extended Kalman filter (EKF) and particle filter (PF). Al Hage *et al.* [19] proposed an optimal thresholding method based on Kullback-Leibury criterion (KLC), which improves Kalman filter and realizes cooperative localization of robots. Zsedrovits *et al.* [20] realized a real-time localization system for unmanned aerial vehicles through airborne cameras and avoidance systems, and useed inertial measurement units and GPS. Ruotsalainen *et al.* [21] introduced the error probability density function in particle filter, and used the model fitting method to verify the measurement error, thus improving the accuracy of multi-sensor fusion localization. Hosseinyalamdary [22] optimized and improved the measurement error of inertial measurement unit through deep Kalman filter. Rodger [23] used Markov fuzzy, statistical, artificial neural network and nearest neighbor prediction methods to analyze multi-sensor indexes and used improved Kalman filter method to reduce noise in the localization system. Li *et al.* [24] converted the measured values of different sensors into a set of measurement matrices, which are solved by improving PHD filtering. Cappello *et al.* [25] implemented a new hybrid controller using fuzzy logic and proportional-integral-derivative (PID) technology and proposed a real-time localization system based on improved unscented Kalman filter.

The contributions of this paper are as follows.

(1) Proposed a multi-sensor fusion localization based on adaptive error correction EKF algorithm to improve the real-time localization accuracy.

(2) Through the contrast adjustment of the sensor detection information, the influence of the error on the estimated value is reduced.

(3) In the two steps of prediction and correction, the normal distribution assumption is carried out twice, so that the predicted value of EKF algorithm is closer to the real value.

(4) Using GA algorithm to optimize EKF algorithm parameters.

The rest of this paper is arranged as follows: Section 2 summarizes the related work; Section 3 performs adaptive error correction on the EKF algorithm; Section 4 performs simulation testing on the improved algorithm; Section 5 summarizes the paper.

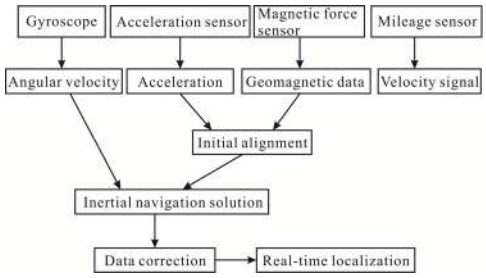

FIGURE 1. Multi-sensor principle based on EKF.

II. PROBLEM DESCRIPTION

The multi-sensor navigation system [26]–[33] of unmanned aerial vehicle (UAV) is taken as the research object in this paper. Its main sensors are gyroscopes, acceleration sensors, magnetic sensors, mileage sensors, etc. The above sensor data is corrected and fused through the Extended Kalman Filter (EKF) algorithm [34]–[40] to obtain the real-time location and attitude information of UAV, as shown in FIGURE 1.

The UAV is a dynamic motion process of six degrees of freedom, and its motion state $\bar{X}$ can be expressed by four elements of location vector $\bar{P}_{et}^{t}$, space motion speed vector $\bar{V}_{et}^{t}$, attitude representation $\bar{q}$ and gyroscope rotation vector $\bar{b}_{\omega}^{t}$ of the space coordinate system.

$$\bar{X} = \begin{bmatrix} \bar{P}_{et}^{t} & \bar{V}_{et}^{t} & \bar{q} & \bar{b}_{\omega}^{t} \end{bmatrix} \tag{1}$$

$\bar{P}_{et}^{t}$, $\bar{V}_{et}^{t}$, $\bar{q}$, and $\bar{b}_{\omega}^{t}$ are obtained as:

$$\begin{cases} \bar{P}_{et}^{t} = \begin{bmatrix} P_x^t & P_y^t & P_z^t \end{bmatrix} \\ \bar{V}_{et}^{t} = \begin{bmatrix} V_x^t & V_y^t & V_z^t \end{bmatrix} \\ \bar{q} = \begin{bmatrix} q_0 & q_1 & q_2 & q_3 \end{bmatrix} \\ \bar{b}_{\omega}^{t} = \begin{bmatrix} b_{\omega x}^t & b_{\omega y}^t & b_{\omega z}^t \end{bmatrix} \end{cases} \tag{2}$$

Considering that ambient noise of the four elements in the space motion velocity vector and the attitude representation when the sensor collected data, it is necessary to perform noise reduction processing first.

$$\begin{cases} \hat{V}_{et}^{t} = D_b^f \bar{f}^b + \bar{g}^t + D_b^t \bar{\delta}_a^b \\ \hat{q} = \dfrac{1}{2} \Omega \cdot \bar{q} \cdot \left(\bar{\omega}_{ib}^b - \bar{b}_{\omega}^b + \bar{\delta}_{\omega}^b \right)^t \end{cases} \tag{3}$$

where, $\bar{\delta}_a^b$ is the environmental noise when the acceleration sensor is detected, $\bar{f}^b$ is the specific force measurement value, $\bar{\delta}_{\omega}^b$ is the environmental noise when the gyroscope is measured, $\bar{\omega}_{ib}^b$ is the measured value of the gyroscope, and $\bar{b}_{\omega}^b$ is the measurement deviation correction value of the gyroscope. The UAV state representation equation of Equation (1) can be converted into

$$\bar{X} = \begin{bmatrix} \bar{P}_{et}^{t} & \hat{V}_{et}^{t} & \hat{q} & \bar{P}_{\omega}^{t} \end{bmatrix} \tag{4}$$

Set $\bar{\delta} = \begin{bmatrix} \bar{\delta}_{\omega}^{bt} & \bar{\delta}_a^{bt} & \bar{\delta}_b^{bt} \end{bmatrix}$ as system noise, Equation (4) can be simplified to

$$\bar{X} = f(\bar{X}, \bar{U}, \bar{\delta}) \tag{5}$$

Due to the nonlinear characteristics of UAV multi-sensor fusion localization system, Equation (5) must be linearized.

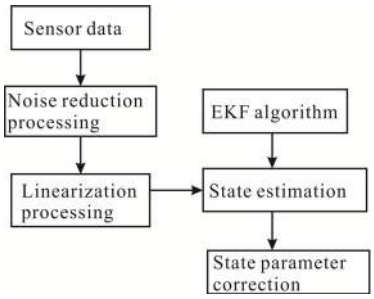

FIGURE 2. EKF-based state estimation flow.

Firstly, Taylor series expansion is used and expressed by Jacobian matrix.

$$\begin{cases} F = \dfrac{\partial f(\bar{X}, \bar{U}, \bar{\delta})}{\partial \bar{X}} \Big| \begin{matrix} \bar{X} = \hat{X}_{k-1} \\ \bar{\delta} = 0 \end{matrix} \\ G = \dfrac{\partial f(\bar{X}, \bar{U}, \bar{\delta})}{\partial \bar{\delta}} \Big| \begin{matrix} \bar{X} = \hat{X}_{k-1} \\ \bar{\delta} = 0 \end{matrix} \\ H = \dfrac{\partial f(\bar{X})}{\partial \bar{X}} \Big| \bar{X} = \hat{X}_{k,k-1} \end{cases} \tag{6}$$

where, F is the external force vector, G is the acceleration vector, and H is the horizontal direction vector.

The motion state can be taken as the state quantity by the location vector $\bar{P}_{et}^{t}$ of the spatial coordinate system, the spatial motion speed vector $\bar{V}_{et}^{t}$, the four elements of the attitude representation $\bar{q}$ and the gyro rotation vector $\bar{b}_{\omega}^{t}$, and the EKF algorithm is used for state estimation to obtain the covariance matrix, which is used to correct the state parameters. The process is shown in FIGURE 2.

Although EKF algorithm can better fuse and locate the data collected by multi-sensors, there are still certain localization errors. Therefore, it is necessary to further optimize it.

III. ADAPTIVE ERROR CORRECTION EKF ALGORITHM

A. CONTRAST AND ADJUSTMENT OF PARAMETER ERROR

Due to the system noise in the process of multi-sensor fusion localization, there is a certain error between the state estimation value and the actual value of EKF algorithm. Therefore, this paper compares and adjusts the information detected by sensors to reduce the influence of the error on the estimation value.

If the error of the state estimation value is W_t, it can be expressed as:

$$W_t = \hat{X}_t - Z_{t,t-1}\bar{X}_{t-1} \tag{7}$$

where, Z is the state transition matrix of the system, the error of the t time state estimation system is obtained to be

$$W_t = G_t\hat{X}_t - g_t \tag{8}$$

where, g_t is the observation value of the t time and G_t is the observation matrix of the state estimation system. Adding an adaptive adjustment factor σ_t to dynamically adjust the weight of the state observation parameters of the system

$$\begin{cases} W_t = -\bar{P}_t \cdot \eta_t \\ W_{x_t} = \dfrac{1}{\sigma} P_{x_t} G_t^T \cdot \eta_t \end{cases} \tag{9}$$

where, $\bar{P}_t$ is the covariance matrix of the system and η_t is Lagrange multiplier vector. The adaptive adjustment factor σ_t is

$$\sigma_t = \begin{cases} 1, & |\Delta W_t| \le \beta_0 \\ \dfrac{\beta_0}{|\Delta W_t|}\left(\dfrac{\beta_1 - |\Delta W_t|}{\beta_1 - \beta_0}\right), & \beta_0 < |\Delta W_t| \le \beta_1 \\ 0, & \beta_1 < |\Delta W_t| \end{cases} \tag{10}$$

where, β_0 and β_1 are the experience values.

B. DISTRIBUTED ERROR SECONDARY CORRECTION

In order to make the predicted value obtained by EKF algorithm closer to the real value, this paper also assumes that it is normal distribution twice in the two steps of prediction and correction respectively. Set the filtering value of the system is $(\hat{x}_{t-1}, 0)$, the observation value is $g(x_t, v_t)$, and the predicted value is $(\hat{x}_{t,t-1}, 0)$ at t time, then the Taylor expansion is approximately

$$x_t = f(\hat{x}_{t-1}, 0) + M_{t-1}\tilde{x}_{t-1} + N_{t-1}w_{t-1} \tag{11}$$

$$g_t = g(\hat{x}_{t,t-1}, 0) + O_t\tilde{x}_{t,t-1} + Q_t v_t \tag{12}$$

The sum of M_{t-1}, N_{t-1}, O_t, and Q_t are Jacobian matrices, and their values are obtained by

$$M_{t-1} = \frac{\partial f_{t-1}}{\partial \hat{x}_{t-1}} = \frac{\partial f(x_{t-1}, w_{t-1})}{\partial x_{t-1}} \Big| (x_{t-1}, w_{t-1}) = (\hat{x}_{t-1}, 0) \tag{13}$$

$$N_{t-1} = \frac{\partial f_{t-1}}{\partial \hat{w}_{t-1}} = \frac{\partial f(x_{t-1}, w_{t-1})}{\partial w_{t-1}} \Big| (x_{t-1}, w_{t-1}) = (\hat{x}_{t-1}, 0) \tag{14}$$

$$O_t = \frac{\partial g_t}{\partial \hat{x}_{t,t-1}} = \frac{\partial g(x_t, v_t)}{\partial x_t} \Big| (x_t, v_t) = (\hat{x}_{t,t-1}, 0) \tag{15}$$

$$Q_t = \frac{\partial g_t}{\partial \hat{v}_{t,t-1}} = \frac{\partial g(x_t, v_t)}{\partial v_t} \Big| (x_t, v_t) = (\hat{x}_{t,t-1}, 0) \tag{16}$$

Then, in the prediction phase of the EKF algorithm, the error covariance matrix $P_{t,t-1}$ predicted by the EKF algorithm is

$$P_{t,t-1} = M_{t-1}P_{t-1}M_{t-1}^T + N_{t-1}Q_{t-1}N_{t-1}^T \tag{17}$$

Then the gain matrix of the state estimation system can be expressed as

$$Y_t = P_{t,t-1}H_t^T\left(H_tP_{t,t-1}H_t^T\right)^{-1} + R_t \tag{18}$$

where, R_t is the probability matrix of the system. In the correction phase of the EKF, error correction is performed on the system observation values

$$\tilde{W}_t = W_t g \cdot x_{t,t-1} \tag{19}$$

The system state prediction equation can be expressed as

$$\hat{x}_t = \hat{x}_{t,t-1} + Y_t \cdot \tilde{W}_t \tag{20}$$

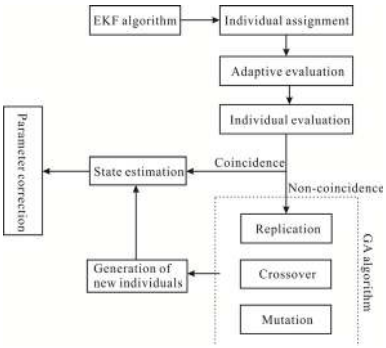

FIGURE 3. Parameter optimization process of EKF algorithm based on GA.

C. PARAMETER OPTIMIZATION OF EKF ALGORITHM BASED ON GA

In order to quickly and accurately find the optimal value of EKF algorithm parameters P_t, G_t, and W_t, this paper introduces Genetic Algorithm (GA) to find the optimal value of EKF algorithm.

Taking EKF algorithm parameters P_t, G_t, and W_t as individuals of GA algorithm, and setting the absolute value ρ of the difference between EKF estimation value and real value as the standard of measurement performance, the smaller the ρ, the more accurate the prediction value of EKF algorithm and the smaller the localization error of the system.

The parameter optimization process of EKF algorithm based on GA is shown in FIGURE 3.

Firstly, the individual is initialized, i.e. the parameters P_t, G_t, and W_t are assigned values. Then, according to the absolute value of the difference between EKF estimation value and real value, the adaptability is obtained to realize individual evaluation. Through the replication, crossover and mutation processes of GA algorithm, parameter iteration is carried out, and evaluation function ρ values are compared to obtain the parameter P_t, G_t and W_t When ρ is the smallest.

IV. PERFORMANCE SIMULATION

In order to verify the algorithm proposed in this paper, the performance simulation of the improved EKF algorithm is carried out in the environment of experiment 1. Set the sampling period is $T = 0.2$, the total number of simulations is $N = 50$, the random number [0, 1] of environmental noise $\bar{\delta}_a^b$ when the acceleration sensor detects and the random number [0, 2] of environmental noise $\bar{\delta}_\omega^b$ when the gyroscope detects, and randomly set two localization targets D1 and D2.

A. EKF ALGORITHM SIMULATION TEST

The comparison results of EKF-based state parameter estimation values are shown in FIGURE 4 and FIGURE 5.

From the results in Figure 4, the parameter estimation tends to the actual value and its error is reduced.

In the above experiment, the multi-sensor fusion localization error is counted, and the results are shown in FIGURE 5.

From the results of simulation experiments, although EKF algorithm can better fuse and locate the data collected by multi-sensors, better fit between actual and estimated values, there are still certain localization errors.

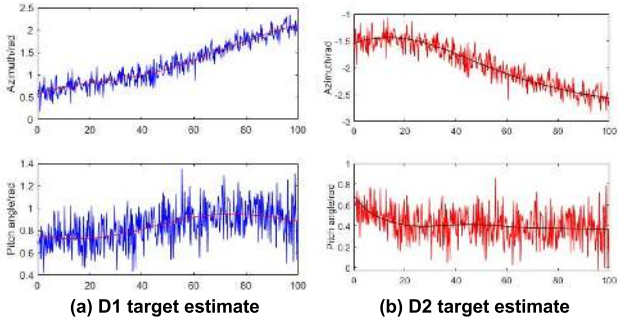

FIGURE 4. Comparison results of estimated state parameters of localization targets.

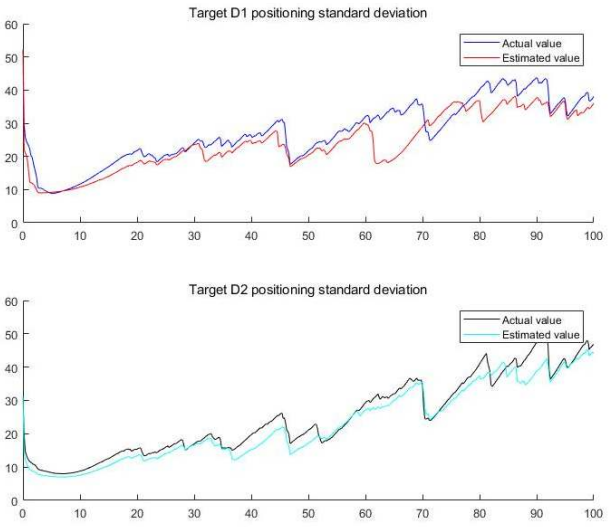

FIGURE 5. Error results of multi-sensor fusion localization.

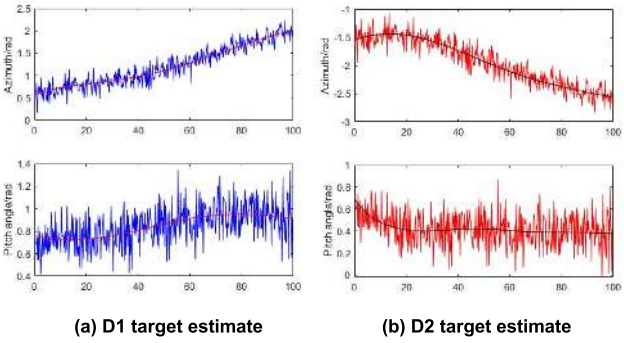

FIGURE 6. Comparison results of estimated state parameters of localization targets.

B. RESULTS WITH PARAMETER ERROR COMPARISON AND ADJUSTMENT

After the standard EKF is optimized by parameter error comparison adjustment proposed in this paper, the comparison results of state parameter estimation values are shown in FIGURE 6.

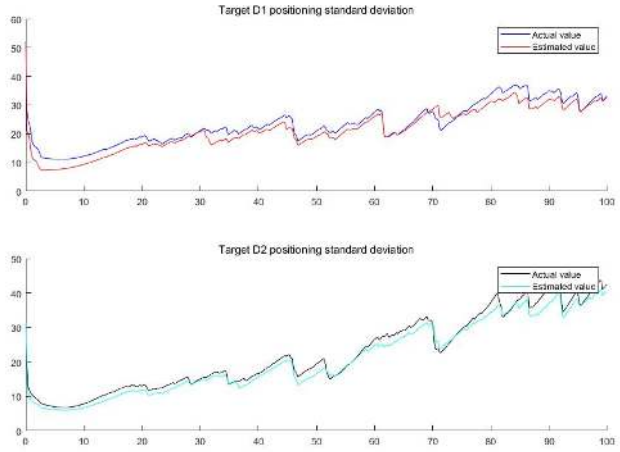

FIGURE 7. Error results of multi-sensor fusion localization.

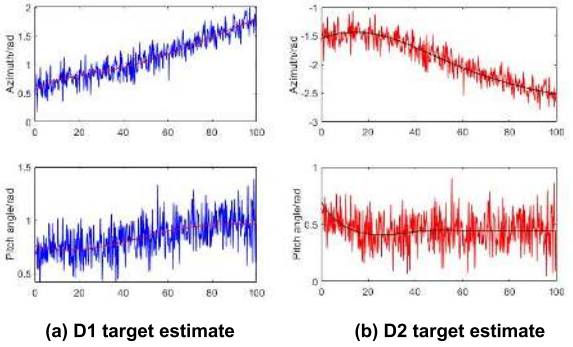

FIGURE 8. Comparison results of estimated state parameters of localization targets.

From the results in Figure 6, the parameter estimation tends to the actual value and its error is reduced.

The error result of multi-sensor fusion localization is shown in FIGURE 7.

As the information detected by the sensor is compared and adjusted, the influence of the error on the estimated value is reduced, so the localization error is reduced by comparing the results of FIGURE 7 and FIGURE 5.

C. RESULTS WITH DISTRIBUTED ERROR SECONDARY CORRECTION

Based on parameter error comparison and adjustment, the optimization is carried out through the distributed error secondary correction strategy proposed in this paper, and the comparison results of state parameter estimation values are shown in FIGURE 8.

From the results in Figure 8, the parameter estimation tends to the actual value and its error is reduced.The error result of multi-sensor fusion localization is shown in FIGURE 9.

Since the normal distribution assumption is carried out twice in the prediction and correction steps, the predicted value obtained by the improved EKF algorithm is closer to the real value. Compared with the results of FIGURE 9 and FIGURE 7, the localization accuracy is further enhanced.

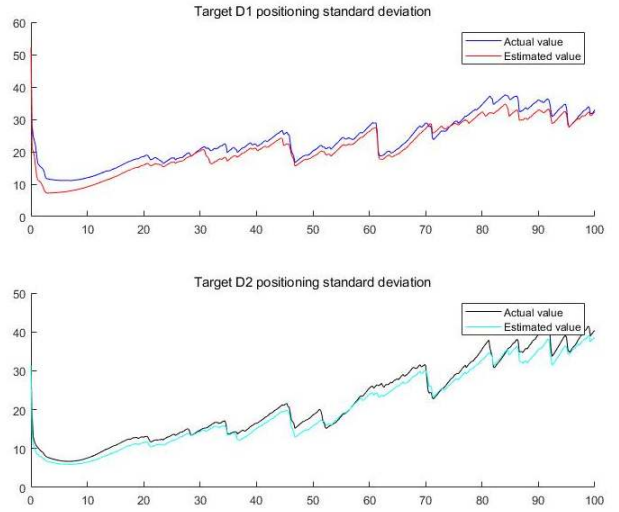

FIGURE 9. Error results of multi-sensor fusion localization.

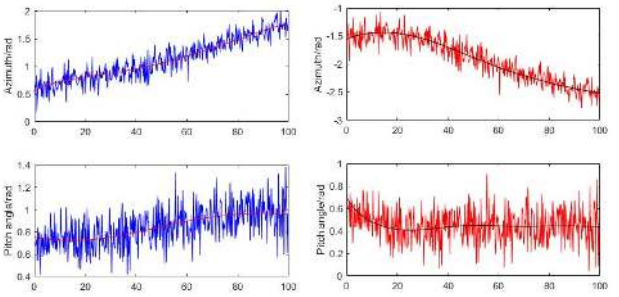

FIGURE 10. Comparison results of state parameter estimation values of localization targets.

D. RESULTS WITH GA PARAMETER OPTIMIZATION

Based on distributed error secondary correction, the optimization is carried out through the GA-based parameter optimization processing strategy proposed in this paper, and the comparison results of state parameter estimation values are shown in FIGURE 10.

From the results in Figure 10, the parameter estimation tends to the actual value and its error is reduced.

The error result of multi-sensor fusion localization is shown in FIGURE 11.

As GA algorithm is used to optimize the parameters, the multi-sensor fusion localization error is further reduced. Comparing the results of FIGURE 11 and FIGURE 9, the improved algorithm has better localization accuracy.

V. UAV REAL-TIME LOCALIZATION TEST

In order to verify the application effect of the improved algorithm in the actual system, this paper constructs a multi-sensor UAV real-time localization system for simulation tests. The UAV sensor MCU uses STM32F405 chip, the inertial measurement unit uses MPU6050 chip (integrating accelerometer and gyroscope at the same time), and the

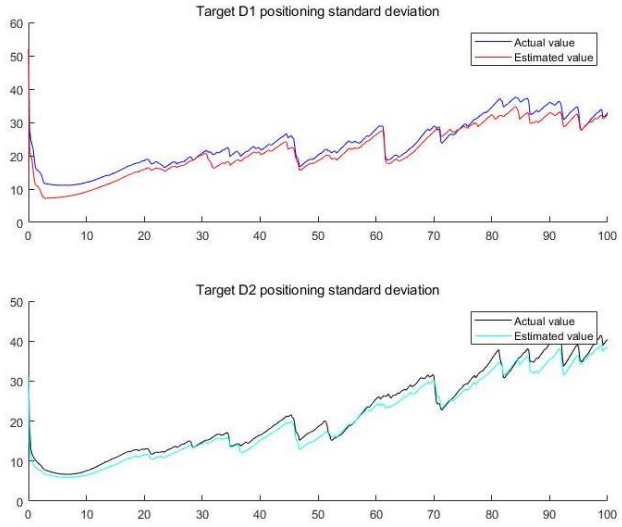

FIGURE 11. Error results of multi-sensor fusion localization.

TABLE 1. Statistics of experimental environment 1.

Time/s	Position Error/%	Standard Deviation/m X	Y
1	0.0020	0.0083	0.0997
50	0.0675	0.1742	0.1480
100	0.6357	0.2964	0.2461
150	0.2002	0.2148	0.3071
200	0.1624	0.1298	0.2863
250	0.2322	0.1469	0.2087
300	0.2250	0.1186	0.1455
350	0.1543	0.2378	0.1534
400	0.2008	0.2033	0.1980
450	0.0744	0.1345	0.2798
500	0.1750	0.1162	0.1920

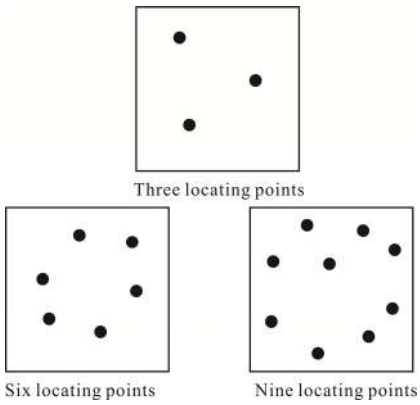

FIGURE 12. Schematic diagram of experimental environment.

magnetometer uses LSM303D chip. The state estimation equation shown in Equation (1) is constructed, and 5, 10 and 15 localization points are respectively set in the experimental area (10 × 10) (FIGURE 12).

TABLE 2. Statistics of experimental environment 2.

Time/s	Position Error/%	Standard Deviation/m X	Y
1	0.0285	0.0993	0.0118
50	0.1263	0.1352	0.2026
100	0.2189	0.2022	0.2579
150	0.0693	0.1949	0.1162
200	0.2196	0.2842	0.1044
250	0.5768	0.2998	0.1309
300	0.4031	0.2539	0.1776
350	0.3489	0.1686	0.1174
400	0.2699	0.1447	0.1262
450	0.0278	0.1334	0.1362
500	0.2678	0.1627	0.1745

TABLE 3. Statistics of experimental environment 3.

Time/s	Position Error/%	Standard Deviation/m X	Y
1	0.0211	0.0818	0.0575
50	0.1842	0.1791	0.1429
100	0.1573	0.2883	0.1512
150	0.1956	0.2973	0.0993
200	0.3827	0.2926	0.1460
250	0.4337	0.1907	0.1315
300	0.4404	0.1639	0.1827
350	0.2879	0.1148	0.1476
400	0.0451	0.1204	0.1060
450	0.2324	0.1352	0.1142
500	0.2831	0.1819	0.1306

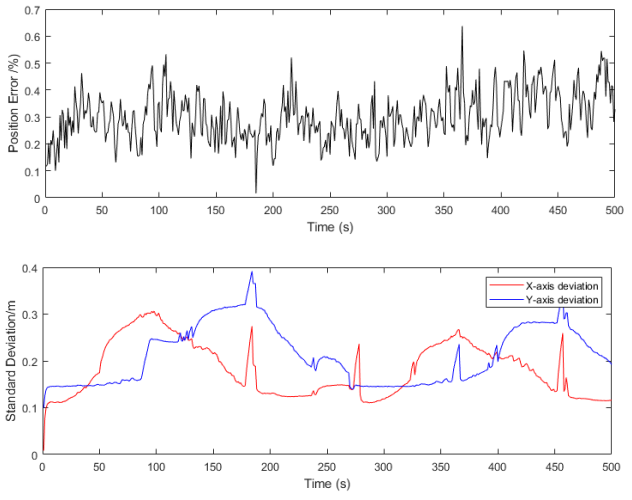

FIGURE 13. Simulation test results of experimental environment 1.

In the experimental environment 1, the actual localization error statistical results of the improved EKF algorithm proposed in this paper are as follows.

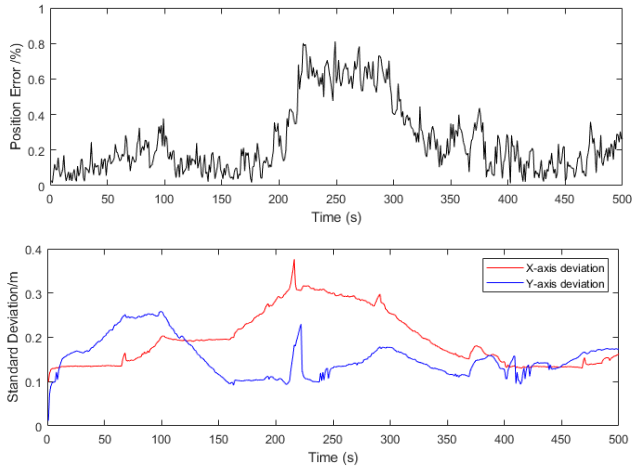

FIGURE 14. Simulation test results of experimental environment 2.

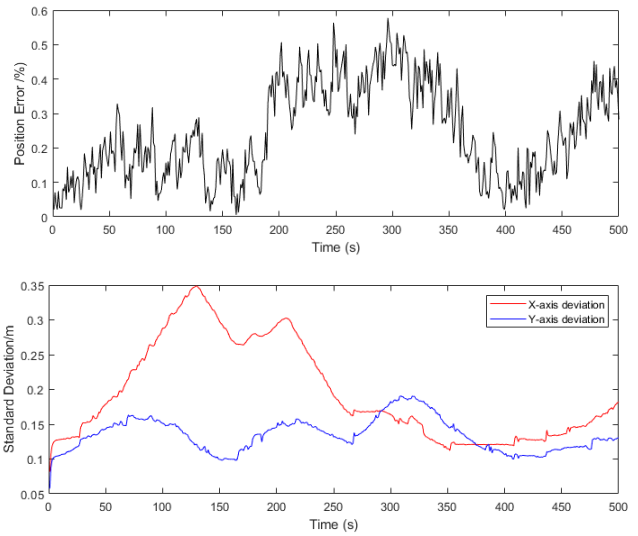

FIGURE 15. Simulation test results of experimental environment 3.

In the experimental environment 2, the actual localization error statistical results of the improved EKF algorithm proposed in this paper are as follows.

In the experimental environment 3, the actual localization error statistical results of the improved EKF algorithm proposed in this paper are as follows.

From the results of Figure 13 and table 1, the average positioning error is 0.1936 for three positioning points, 0.2324 for six positioning points and 0.2421 for nine positioning points. Therefore, the following conclusions can be drawn, with the continuous increase of localization points, the improved algorithm proposed in this paper still maintains a certain localization accuracy and has strong robustness.

VI. CONCLUSION

The traditional single sensor localization method cannot meet the requirements of high precision and high reliability for moving objects. However, the fusion localization method based on multi-sensor information avoids the deficiency of single sensor and has been studied and applied more and more. In this paper, a multi-sensor fusion localization method based on adaptive error correction EKF algorithm is proposed to solve the problem that the standard extended Kalman filter algorithm has large errors in UAV multi-sensor fusion localization. Experimental simulation results show that the improved algorithm proposed in this paper has higher real-time localization accuracy and higher robustness than the standard EKF algorithm.

REFERENCES

[1] P. Dabove and V. Di Pietra, "Towards high accuracy GNSS real-time positioning with smartphones," *Adv. Space Res.*, vol. 63, no. 1, pp. 94–102, Jan. 2019.

[2] F. M. Jumaah, A. A. Zadain, B. B. Zaidan, A. K. Hamzah, and R. Bahbibi, "Decision-making solution based multi-measurement design parameter for optimization of GPS receiver tracking channels in static and dynamic real-time positioning multipath environment," *Measurement*, vol. 118, pp. 83–95, Mar. 2018.

[3] Z. Xie, W. Guan, J. Zheng, X. Zhang, S. Chen, and B. Chen, "A high-precision, real-time, and robust indoor visible light positioning method based on mean shift algorithm and unscented Kalman filter," *Sensors*, vol. 19, no. 5, p. 1094, 2019.

[4] M. Kim and K.-D. Park, "Development and positioning accuracy assessment of single-frequency precise point positioning algorithms by combining GPS code-pseudorange measurements with real-time SSR corrections," *Sensors*, vol. 17, no. 6, p. 1347, 2017.

[5] M. Chiputa and L. Xiangyang, "Real time Wi-Fi indoor positioning system based on RSSI measurements: A distributed load approach with the fusion of three positioning algorithms," *Wireless Pers. Commun.*, vol. 99, no. 1, pp. 67–83, Mar. 2018.

[6] P. Dabove and V. Di Pietra, "Single-baseline RTK positioning using dual-frequency GNSS receivers inside smartphones," *Sensors*, vol. 19, no. 19, p. 4302, 2019.

[7] W. Gao, S. Pan, C. Gao, Q. Wang, and R. Shang, "Tightly combined GPS and GLONASS for RTK positioning with consideration of differential inter-system phase bias," *Meas. Sci. Technol.*, vol. 30, no. 5, May 2019, Art. no. 054001.

[8] F. Hu and C. Tu, "An optimization model for target tracking of mobile sensor network based on motion state prediction in emerging sensor networks," *J. Intell. Fuzzy Syst.*, vol. 32, no. 5, pp. 3509–3524, Apr. 2017.

[9] A. El-Mowafy and N. Kubo, "Integrity monitoring of vehicle positioning in urban environment using RTK-GNSS, IMU and speedometer," *Meas. Sci. Technol.*, vol. 28, no. 5, May 2017, Art. no. 055102.

[10] D. Ghosh, B. Samanta, and D. Chakravarty, "Multi sensor data fusion for 6D pose estimation and 3D underground mine mapping using autonomous mobile robot," *Int. J. Image Data Fusion*, vol. 8, no. 2, pp. 173–187, Apr. 2017.

[11] D. Nada, M. Bousbia-Salah, and M. Bettayeb, "Multi-sensor data fusion for wheelchair position estimation with unscented Kalman filter," *Int. J. Autom. Comput.*, vol. 15, no. 2, pp. 207–217, Apr. 2018.

[12] A. Belmonte-Hernandez, G. Hernandez-Penaloza, F. Alvarez, and G. Conti, "Adaptive fingerprinting in multi-sensor fusion for accurate indoor tracking," *IEEE Sensors J.*, vol. 17, no. 15, pp. 4983–4998, Aug. 2017.

[13] G. Shivanand, K. V. K. Reddy, and D. Prasad, "An innovative asynchronous, multi-rate, multi-sensor state vector fusion algorithm for air defence applications," *IFAC-PapersOnLine*, vol. 49, no. 1, pp. 337–342, 2016.

[14] G. Muniandi and E. Deenadayalan, "Train distance and speed estimation using multi sensor data fusion," *IET Radar, Sonar Navigat.*, vol. 13, no. 4, pp. 664–671, Apr. 2019.

[15] M. K. Al-Sharman, B. J. Emran, M. A. Jaradat, H. Najjaran, R. Al-Husari, and Y. Zweiri, "Precision landing using an adaptive fuzzy multi-sensor data fusion architecture," *Appl. Soft Comput.*, vol. 69, pp. 149–164, Aug. 2018.

[16] S. Plangi, A. Hadachi, A. Lind, and A. Bensrhair, "Real-time vehicles tracking based on mobile multi-sensor fusion," *IEEE Sensors J.*, vol. 18, no. 24, pp. 10077–10084, Dec. 2018.
[17] S. Kumar and R. M. Hegde, "Multi-sensor data fusion methods for indoor localization under collinear ambiguity," *Pervas. Mobile Comput.*, vol. 30, pp. 18–31, Aug. 2016.
[18] J. Gabela, A. Kealy, S. Li, M. Hedley, W. Moran, W. Ni, and S. Williams, "The effect of linear approximation and Gaussian noise assumption in multi-sensor positioning through experimental evaluation," *IEEE Sensors J.*, vol. 19, no. 22, pp. 10719–10727, Nov. 2019.
[19] J. Al Hage, M. E. El Najjar, and D. Pomorski, "Multi-sensor fusion approach with fault detection and exclusion based on the Kullback–Leibler Divergence: Application on collaborative multi-robot system," *Inf. Fusion*, vol. 37, pp. 61–76, Sep. 2017.
[20] T. Zsedrovits, P. Bauer, A. Hiba, M. Nemeth, B. J. M. Pencz, A. Zarandy, B. Vanek, and J. Bokor, "Performance analysis of camera rotation estimation algorithms in multi-sensor fusion for unmanned aircraft attitude estimation," *J. Intell. Robotic Syst.*, vol. 84, nos. 1–4, pp. 759–777, Dec. 2016.
[21] L. Ruotsalainen, M. Kirkko-Jaakkola, J. Rantanen, and M. Mäkelä, "Error modelling for multi-sensor measurements in infrastructure-free indoor navigation," *Sensors*, vol. 18, no. 2, p. 590, 2018.
[22] S. Hosseinyalamdary, "Deep Kalman filter: Simultaneous multi-sensor integration and modelling; A GNSS/IMU case study," *Sensors*, vol. 18, no. 5, p. 1316, 2018.
[23] J. A. Rodger, "Advances in multisensor information fusion: A Markov–Kalman viscosity fuzzy statistical predictor for analysis of oxygen flow, diffusion, speed, temperature, and time metrics in CPAP," *Expert Syst.*, vol. 35, no. 4, 2018, Art. no. e12270.
[24] T. Li, J. Prieto, H. Fan, and J. M. Corchado, "A robust multi-sensor PHD filter based on multi-sensor measurement clustering," *IEEE Commun. Lett.*, vol. 22, no. 10, pp. 2064–2067, Oct. 2018.
[25] F. Cappello, S. Ramasamy, and R. Sabatini, "A low-cost and high performance navigation system for small RPAS applications," *Aerosp. Sci. Technol.*, vol. 58, pp. 529–545, Nov. 2016.
[26] F. Schilling, J. Lecoeur, F. Schiano, and D. Floreano, "Learning vision-based flight in drone swarms by imitation," *IEEE Robot. Autom. Lett.*, vol. 4, no. 4, pp. 4523–4530, Oct. 2019.
[27] D. Palossi, A. Loquercio, F. Conti, E. Flamand, D. Scaramuzza, and L. Benini, "A 64-mW DNN-based visual navigation engine for autonomous nano-drones," *IEEE Internet Things J.*, vol. 6, no. 5, pp. 8357–8371, Oct. 2019.
[28] J. Yin, P. Hoogeboom, C. Unal, H. Russchenberg, F. van der Zwan, and E. Oudejans, "UAV-aided weather radar calibration," *IEEE Trans. Geosci. Remote Sens.*, vol. 57, no. 12, pp. 10362–10375, Dec. 2019.
[29] F. Fries, S. K. H. Win, E. Tang, J. E. Low, L. S. T. Win, P. V. Y. Alvarado, and S. Foong, "Design and implementation of a compact rotational speed and air flow sensor for unmanned aerial vehicles," *IEEE Sensors J.*, vol. 19, no. 22, pp. 10298–10307, Nov. 2019.
[30] B. Liu, J. Xu, B. Fu, Y. Hao, and T. An, "A covariance shaping filtering method for tightly-coupled MIMU/GNSS of UAV," *Aircr. Eng. Aerosp. Technol.*, vol. 91, no. 10, pp. 1257–1267, Nov. 2019.
[31] Z. Rochala, K. Wojtowicz, P. Kordowski, and B. Brzozowski, "Experimental tests of the obstacles detection technique in the hemispherical area for an underground explorer UAV," *IEEE Aerosp. Electron. Syst. Mag.*, vol. 34, no. 10, pp. 18–26, Oct. 2019.
[32] O. Saif, I. Fantoni, and A. Zavala-Río, "Distributed integral control of multiple UAVs: Precise flocking and navigation," *IET Control Theory Appl.*, vol. 13, no. 13, pp. 2008–2017, Sep. 2019.
[33] P. Fraga-Lamas, L. Ramos, V. Mondéjar-Guerra, and T. M. Fernández-Caramés, "A review on IoT deep learning UAV systems for autonomous obstacle detection and collision avoidance," *Remote Sens.*, vol. 11, no. 18, p. 2144, 2019.
[34] R. Rana, P. Gaur, V. Agarwal, and H. Parthasarathy, "Tremor estimation and removal in robot-assisted surgery using lie groups and EKF," *Robotica*, vol. 37, no. 11, pp. 1904–1921, Nov. 2019.
[35] R. A. Walambe and V. A. Joshi, "Closed loop stability of a PMSM-EKF controller-observer structure," *IFAC-PapersOnLine*, vol. 51, no. 1, pp. 249–254, 2018.
[36] Y. Sun, L. Li, B. Yan, C. Yang, and G. Tang, "A hybrid algorithm combining EKF and RLS in synchronous estimation of road grade and vehicle' mass for a hybrid electric bus," *Mech. Syst. Signal Process.*, vols. 68–69, pp. 416–430, Feb. 2016.
[37] L. de Souza Rosa, A. Dasu, P. C. Diniz, and V. Bonato, "A faddeev systolic array for EKF-SLAM and its arithmetic data representation impact on FPGA," *J. Signal Process. Syst.*, vol. 90, no. 3, pp. 357–369, Mar. 2018.
[38] F. Hu, "Simulation and analysis of airbag parameter variation under different gas flows," *Cluster Comput.*, vol. 22, no. S6, pp. 13235–13245, Nov. 2019.
[39] F. Mwasilu and J.-W. Jung, "Enhanced fault-tolerant control of interior PMSMs based on an adaptive EKF for EV traction applications," *IEEE Trans. Power Electron.*, vol. 31, no. 8, pp. 5746–5758, Aug. 2016.
[40] L. R. Lustosa, S. Pizziol, F. Defaÿ, and J.-M. Moschetta, "An error model of a complementary filter for use in Bayesian Estimation–The CF-EKF filter," *IFAC-PapersOnLine*, vol. 49, no. 17, pp. 444–449, 2016.

FENGJUN HU received the Ph.D. degree in control theory and control engineering from the Zhejiang University of Technology. He was selected as the Second Level Personnel of the 151 Talents Project in Zhejiang Province and as the Outstanding Young Teacher Funding Program for Zhejiang Higher Education Institutions. He has been the Deputy Director of the Scientific Research Department, Zhejiang Shuren University, since 2016, and a Full Professor and the Head of the Department of Human–Computer Interaction, Three-Dimensional Design Laboratory, since 2017. He has published more than 30 articles in important journals such as *Cluster Computing* and *Journal of Intelligent and Fuzzy*, in which more than 20 articles have been included in SCI or EI journals and more than 20 Chinese invention patents have been applied. He has also authorizing more than 20 Chinese utility model patents and more than 40 software copyrights.

GANG WU has been appointed as a Researcher with ACTA. He is also an Expert in bone tissue engineering and advanced medical materials. He has achieved 80 SCI publications in top journals in this field, such as *Biomaterials*, *ACS Applied Materials and Interfaces*, *Cytokine and Growth Factor Reviews*, and *Tissue Engineering and Bone*. He has been an External Reviewer for more than 15 top international journals such as *Nature Communications* and *Biomaterials*.